Vol. 25(1):63-74 | Ocean and Polar Research | March 2003

Article

An Analytical Investigation on the Build-up of the Temperature Field due to a Point Heat Source in Shallow Coastal Water with Oscillatory Alongshore-flow

Kyung Tae Jung*[1], Chong Hak Kim[2], Chan Joo Jang[1], Ho Jin Lee[3], Sok Kuh Kang[1], and Ki Dai Yum[1]

[1]*Coastal and Harbor Engineering Laboratory, KORDI*
Ansan P.O. Box 29, Seoul, Korea
[2]*NETEC, Yuseong-gu, Daejeon, Korea*
[3]*Korea Maritime University, Yeongdo-gu, Busan, Korea*

Abstract : The build-up of the heat field in shallow coastal water due to a point source has been investigated using an analytical solution of a time-integral form derived by extending the solutions by Holley (1969) and also presented in Harleman (1971). The uniform water depth is assumed with non-isotropic turbulent dispersion. The alongshore-flow is assumed to be uni-directional, spatially uniform and oscillatory. Due to the presence of the oscillatory alongshore-flow, the heat build-up occurs in an oscillatory manner, and the excess temperature thereby fluctuates in that course and even in the quasi-steady state. A series of calculations reveal that proper choices of the decay coefficient as well as dispersion coefficients are critical to the reliable prediction of the excess temperature field. The dispersion coefficients determine the absolute values of the excess temperature and characterize the shoreline profile, particularly within the tidal excursion distance, while the decay coefficient determines the absolute value of the excess temperature and the convergence rate to that of the quasi-steady state. Within the e-folding time scale $1/k_d$ (where k_d is the heat decay coefficient), heat build-up occurs more than 90% of the quasi-steady state values in a region within a tidal excursion distance (L), while occurs increasingly less the farther we go to the downstream direction (about 80% at 1.25 L, and 70% at 1.5 L). Calculations with onshore and offshore discharges indicate that thermal spreading in the direction of the shoreline is reduced as the shoreline constraint which controls the lateral mixing is reduced. The importance of collecting long-term records of in situ meteorological conditions and clarifying the definition of the heat loss coefficient is addressed. Interactive use of analytical and numerical modeling is recommended as a desirable way to obtain a reliable estimate of the far-field excess temperature along with extensive field measurements.

Key words : analytical model, heat discharge, excess temperature, point source, oscillatory alongshore-flow, turbulent dispersion.

1. Introduction

Faced with ever-increasing difficulties in selecting sites for new power plants, construction of additional generating units at existing sites has been a viable alternative for long-term power development in Korea. Unfortunately, the plan might have an increasing environmental impact. The increase in the size of the thermal-impact zone would seriously alter the ecosystem and sharpen the discontent of fishery communities. The conflicts among the interested parties have caused serious social concerns over the years. For that reason, various modeling studies were performed (Pukyung University, 1996; KEPCO; 1996; KOPEC, 2002; Kunsan University, 2002) and extensive measurement projects are on going (KORDI, 2002).

Undoubtedly, knowledge on the build-up of the heat

*Corresponding author. E-mail : ktjung@kordi.re.korea

field is essential to the proper interpretation of observations and numerical modeling. Employing the CORMIX system (Cornell Mixing Zone Expert system developed by Jirka and Hinton, 1992) might be a straightforward way to get some basic idea on the spread of thermal heat (Jung *et al.*, 2001). However, the system was designed to provide information mainly on the near-field (and secondly the far-field) at a quasi-steady state in the presence of a steady cross-flow. That is, no information is provided on the transient feature of the heat build-up and the far-field temperature rise in a highly unsteady ambient condition. Assessment of heat build-up problems based on numerical modeling has been commonplace, yet, it still has some inherent limitations; the numerical models are not free from noise and their long-term integration is often very time-consuming.

Analytical methods are obviously advantageous over the numerical methods in that computational cost is much lower and clear insight on the behavior of thermal effects can be obtained, although bathymetry, coastline and ambient conditions must be highly idealized. In realistic cases, a particle tracking model developed by KEPRI (1993) might be a useful alternative.

In this study, an analytical solution of time-integral form will be employed to investigate the build-up of the heat field with emphasis on the far-field temperature. The solution determining the excess temperature due to a point source has been derived by extending the one-dimensional solution derived by Holley (1969) (and also by Harleman (1971)). A series of calculations are then carried out to examine the time scales required for the heat field to reach a quasi-steady state, effects of the onshore and offshore discharges and cross-flow intensity, especially the role of turbulent dispersion and heat loss.

2. Model equation and solution

We consider a horizontally unbounded, shallow open sea with constant water depth where the flow is time-varying but uni-directional and furthermore turbulent dispersion is non-isotropic. Under these assumptions, the heat balance equation may be written in the following form (Atkins and Driver, 1975):

$$\frac{\partial T}{\partial t} + u\frac{\partial T}{\partial x} = k_x\frac{\partial^2 T}{\partial x^2} + \frac{k_x}{\alpha^2}\frac{\partial^2 T}{\partial y^2} - k_d T, \tag{1}$$

where t is time, x, y are the cartesian coordinates, T is the excess temperature, u is the x-directed flow velocity, k_x, k_x/α^2 are the horizontal dispersion coefficients and k_d is a heat decay coefficient. The last term on the right hand side of equation (1) represents the heat loss to the atmosphere. See appendix for the detailed derivation of equation (1) governing the excess temperature field and the underlying assumption related with its use.

The alongshore-flow is assumed to compose an oscillatory current as given:

$$u(t) = U_{\max}\sin\omega t, \tag{2}$$

where $U_{\max}$ is the amplitude of the oscillatory current, $\omega(=2\pi/T_p)$ is the angular frequency of the oscillatory current (T_p is the period). $U_{\max}$ is the space-invariant so that u considered in this study as a function of time only.

Atkins and Driver (1975) presented a set of analytical solutions in an integral form, solutions in a uniform, mean flow (that is, with U_m) with assumption of point and line sources, and an approximate solution at the quasi-steady level in a uniform, oscillatory flow by assuming that a source is distributed over a tidal excursion length (from $x=-L/2$ to $+L/2$) in the form $1/\sqrt{(L/2)^2-x^2}$ (where L is the tidal excursion length). Holley (1969) and Harleman (1971) derived a one-dimensional solution to the time-integral form in the presence of mean and oscillatory flows on the basis of the solution by Carter and Okubo (1965) due to an instantaneous source. Okubo (1967) and Yasuda (1982) examined time-varying shear effects using the vertically two-dimensional model (that is, $x-z$ model) by calculating various moments of concentration distribution due to instantaneous sources. For the present study, the solution is extended to a two-dimensional form to get an information on the full-time evolution of the heat buildup, including solutions at the quasi-steady state as well as the initial transient. The extension is straightforward and closely follows the procedure used by Harleman (1971).

Two transformations are required. Firstly, a new concentration variable is introduced such that

$$T = Ce^{-k_d(t-\tau)}. \tag{3}$$

Secondly, χ, a longitudinal distance moving with the velocity, is introduced. That is,

$$\chi = x - \int_\tau^t u(t)dt. \tag{4}$$

With the above two transformations, equation (1) reduces to

$$\frac{\partial C}{\partial t} = k_x\frac{\partial^2 C}{\partial \chi^2} + \frac{k_x}{\alpha^2}\frac{\partial^2 C}{\partial y^2}, \tag{5}$$

which is an elementary form of the diffusion equation. An appropriate solution of equation (5) to an instantaneous release of heat at the origin (0, 0) at time $t = \tau$ is then

$$C = \frac{\alpha}{4\pi k_x(t-\tau)} \cdot \exp\left[-\frac{\chi^2 + (\alpha y)^2}{4k_x(t-\tau)}\right], \quad (6)$$

which is often called the unit-impulse response function in the literature. For the solutions in three-dimensions and other source conditions, see Carslaw and Jaeger (1959) and Cussler (1984).

Equation (6) can be written in terms of the original temperature variable as follows:

$$C = \frac{\alpha}{4\pi k_x(t-\tau)} \cdot \exp\left[-\frac{\chi^2 + (\alpha y)^2}{4k_x(t-\tau)} - k_d(t-\tau)\right]. \quad (7)$$

The solution in terms of the original coordinate can be, though omitted here, obtained using the following relation:

$$\chi = x + U_{\max}/\omega \cdot (\cos\omega t - \cos\omega\tau). \quad (8)$$

Once the unit-impulse response function is defined, the convolution integral can be applied for the continuous release. Let the rate of heat supply be qT_o/h, in which q is the discharge flow rate and h is water depth, and the heat release starts at $t = 0$. The excess water temperature in the original space coordinate is then given by

$$T = \int_0^t \frac{\alpha q T_o}{4\pi h k_x(t-\tau)} \cdot I(x, y, t, \tau) \cdot e^{-k_d(t-\tau)} d\tau \quad (9)$$

where

$$I = \exp\left[-\frac{\{x + U_{\max}/\omega \cdot (\cos\omega t - \cos\omega\tau)\}^2 + (\alpha y)^2}{4k_x(t-\tau)}\right]. \quad (10)$$

In this case, the source is located at (x_o, y_o),

$$I = \exp\left[-\frac{\{x - x_o + U_{\max}/\omega \cdot (\cos\omega t - \cos\omega\tau)\}^2 + \alpha(y - y_o)^2}{4k_x(t-\tau)}\right]. \quad (11)$$

The integral of equation (9) needs to be evaluated numerically. A simple mid-ordinate method has been used in this study.

3. Applications

In applications described below, we consider a semi-infinite ocean, that is, coastal water with a coastline located at $y = 0$. The positive y is directed to the offshore (on the western part of the coastline), and the positive x is directed to the south, assumed to be parallel to the coastline and the alongshore flow (in fact, the direction of the x coordinate does not affect the result due to the symmetry of solutions). The excess temperature field in the semi-infinite ocean is simply obtained by introducing an image source at $(x_o, -y_o)$. In detail,

$$T = \int_0^t \frac{\alpha q \Delta T_o}{4\pi h k_x(t-\tau)} \cdot I(x - x_o, y - y_o, t, \tau) \cdot e^{-k_d(t-\tau)} d\tau + \int_0^t \frac{\alpha q \Delta T_o}{4\pi h k_x(t-\tau)} \cdot I(x - x_o, y + y_o, t, \tau) \cdot e^{-k_d(t-\tau)} d\tau. \quad (12)$$

The multiple sources can be dealt with by applying a linear superposition.

Following Hydraulics Research Station (1978), the longitudinal dispersion coefficient is defined as follows:

$$k_x = \theta h U_{\max}, \quad (13)$$

where θ is known to range from 0.6 to 8.7 according to Talbot's report (1973). The values of the lateral dispersion coefficient are changed by taking a range of values of α^2. Hydraulics Research Station (1975) used $\alpha^2 = 1.75$ as a preferred value.

A series of calculations are to be carried out in this study with emphasis on the role of dispersion and heat loss coefficients. To facilitate the sensitivity calculations, we here define the *base combination of* the input parameters as follows: $h = 7$ m; $q = 218$ m^3/s; $T_o = 8.3$°C; $U_{\max} = 0.8$ m/s; $T_p = 12.45$ hours; $\theta = 8.4$; $\alpha = 1.0$ and $k_d = 0.1065 \times 10^{-5}$s^{-1}. The source location (x_o, y_o) is taken as (0, 150 m). The time increment is approximated to a finite value $\Delta\tau$ and is chosen as 1/3600 seconds.

For the sake of convenience, results to be presented below are all normalized by the excess temperature at the source, that is, T_o, and the shoreline and offshore distances are normalized by the tidal excursion distance, L, which is given by $U_{\max}T_p/\pi$. For the case $U_{\max} = 0.8$ m/s, the excursion distance is about 11.4 km and is denoted by $L_{0.8}$.

Convergence of the excess temperature to a quasi-steady state

One of the basic questions frequently raised in thermal studies is how fast the heat build-up occurs and how much time is needed to reach a quasi-steady state. Due to the presence of the oscillatory shoreline-flow, the heat build-

up occurs in an oscillatory manner and the excess temperature thereby fluctuates in that course and even in the quasi-steady state.

Initially, a calculation is performed over 100 lunar days with the use of the base combination of input parameters. Fig. 1 shows the time variations in the maximum (solid lines) and minimum (dashed lines) values of the excess temperature occurring within an M_2 tidal cycle at five positions $(x, y) = (0.75\,L_{0.8}, 150\text{ m})$, $(1.0\,L_{0.8}, 150\text{ m})$, $(1.25\,L_{0.8}, 150\text{ m})$ and $(1.5\,L_{0.8}, 150\text{ m})$, aligned parallel with the shoreline. It is shown that both the maximum and minimum values of the excess temperature at all positions converges on quasi-steady state values in a similar manner. The difference between the maximum and minimum excess temperature is largest at the position $(0.75\,L_{0.8}, 150\text{ m})$, approximately seven and three times larger than those at the positions of $(1.5\,L_{0.8}, 150\text{ m})$ and $(1.25\,L_{0.8}, 150\text{ m})$, respectively. That is, the fluctuation of the excess temperature due to the oscillatory flow is much more pronounced at the near-field than at the far-field.

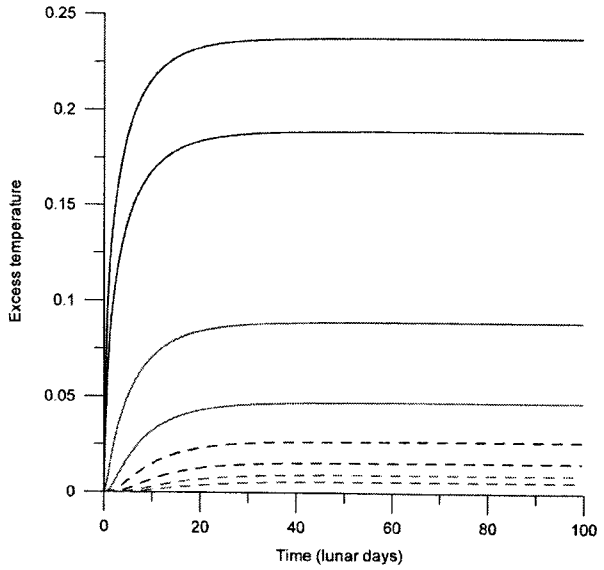

Fig. 1. Time variations in the maximum (solid lines) and minimum (dashed lines) values of the excess temperature occurring within an M_2 tidal cycle at positions $(x, y) = (0.75\,L_{0.8}, 150\text{ m})$ (blue), $(1.0\,L_{0.8}, 150\text{ m})$ (black), $(1.25\,L_{0.8}, 150\text{ m})$ (green) and $(1.5\,L_{0.8}, 150\text{ m})$ (red).

In Fig. 1, we can see that the heat build-up initially occurs at a very rapid rate and slows down as time goes by. Roughly speaking, the heat build-up occurs for the most part within 15 days.

As a way of assessing the rate of heat build-up in a more rigorous manner, we have checked the time that the maximum excess temperature reaches 70%, 80%, 90% and 95% of the quasi-steady state value (chosen as the value of the maximum excess temperature at 100 lunar days). Table 1 summarizes the results.

It is more evident from Table 1 that the positions close to the source experience a faster build-up than the far-field positions. The heat field within a tidal excursion distance reaches 90% of the quasi-steady state value in about 10 days, while going beyond the tidal excursion distance over a significantly longer time. It is implied that the far-field is in reality hardly in a quasi-steady state because the variation in the meteorological conditions and the interaction with the offshore water frequently occurs in significantly shorter time scales.

Comparison with the time scale derived from the initial value problem in the absence of the convection and turbulent dispersion might be of value. Neglecting the convection and dispersion terms, we get a solution in the form

$$T(t) = T(0)e^{-k_d t} \tag{14}$$

where $T(0)$ is the initial temperature. Note that $1/k_d$ is the

Table 1. Time required for the maximum excess temperature at four positions to reach certain percentages of the quasi-steady state value.

$\frac{T_{max}(\,,t)}{T_{max}(\,,t_{qs})}$ (in %)	Elapsed time (in lunar days)			
	$(0.75\,L_{0.8}, 150\text{ m})$	$(1.00\,L_{0.8}, 150\text{ m})$	$(1.25\,L_{0.8}, 150\text{ m})$	$(1.50\,L_{0.8}, 150\text{ m})$
70	3.2	4.1	7.5	10.7
80	5.4	6.4	10.3	13.8
90	9.7	10.7	15.3	19.3
95	14.3	15.7	20.8	25.2

Note: t_{qs} denotes 100 lunar days.

e-folding time scale characterizing the rate of convergence (in case the heat release suddenly stops), which is equal to 10.5 lunar days in the case of $k_d = 0.1065\times10^{-5}$/s. We note that, within the e-folding time scale, the heat build-up occurs up to 90% of the quasi-steady state values in a region within a tidal excursion distance, about 80% at (1.25 $L_{0.8}$, 150 m), and about 70% at (1.5 $L_{0.8}$, 150 m).

In the literature of thermal modeling studies, some researchers reported results based on calculations continued only about 3 to 5 days (for example, the application of a two-dimensional model by KEPRI (1993)). In that case, the predicted excess temperature is obviously far different from the quasi-steady state value even in regions close to near-field. The time scales presented in Table 1 are fairly comparable with those obtained via a particle tracking model (KEPRI, 1993).

It is worthwhile to note that changes in the excess temperature in the interval between (1.0 $L_{0.8}$, 150 m) and (1.25 $L_{0.8}$, 150 m) are significantly larger than those of other intervals. In such cases, we display the instantaneous shoreline distribution of the excess temperature as Fig. 2, which includes the alongshore distributions at four different times of the 200 lunar tidal cycle (in detail, at $t = 199T_p$, $+ (4/16)\pi/T_p$, when u reaches a positive maximum, $t = 199T_p + (6/16)\pi/T_p$, $t = 199T_p + (8/16)\pi/T_p$ when u becomes zero and, for comparison purposes, $t = 199T_p + (9/16)\pi/T_p$ when u has a small negative value). We can see that, as the heat is carried downstream by the shoreline-flow (physically,

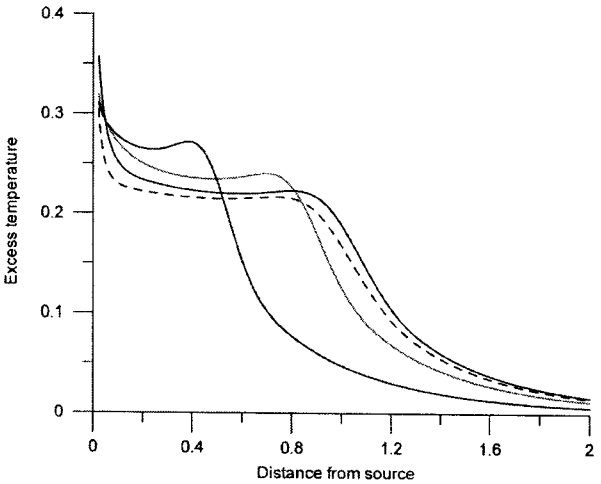

Fig. 2. The instantaneous alongshore distributions of the excess temperature at the four successive time steps of the 200th lunar tidal cycle ($t = 199T_p + (4/16)\pi/T_p$ (blue), $t = 199T_p + (6/16)\pi/T_p$ (green), $t = 199T_p + (8/16)\pi/T_p$ (black solid), and $t = 199T_p + (9/16)\pi/T_p$) (black dashed).

when the source is moving up to $x = L_{0.8}$), the maximum excess temperatures successively appear. In the course of this, the shoreline profile of the excess temperature remains more or less the same, retaining the same form with a moderate change on the upstream side (except for the source region) and with a rapid decrease on the immediate downstream side. Consequently, the rapid change in the maximum excess temperature occurs in the region between (1.0 $L_{0.8}$, 150 m) and (1.25 $L_{0.8}$, 150 m). This feature has been expected because convection plays a major role in the heat field build-up within the tidal excursion distance, while the dispersion process dominantly acts beyond the distance. On the bulge-like form of the alongshore profile downstream, especially noted at $t = 199T_p + (4/16)\pi T_p$, discussion will be made later with regards to the effects of turbulent dispersion coefficients.

Effects of moving the source point in an offshore direction

As a countermeasure to reduce thermal impact on the coastal environment, offshore discharge is often considered instead of the surface discharge at the shore. Construction of a jetty introduced as a countermeasure at the end of the discharge channel of Youngkwang nuclear power plant (KOPEC, 2001) is partly based on the idea of moving the source position to the offshore side. The effects of moving the source position to the offshore direction is here examined. Furthermore, even in the case of surface discharge, choosing a proper source position is a non-trivial subject in analytical modeling, since the discharged heated water usually enters the coastal waters with a certain degree of momentum and then is deflected somewhere offshore by the action of the ambient shoreline-flow.

Fig. 3 shows the distribution of the maximum excess temperature at the cross section of $x = L_{0.8}$ computed for $t = 199T_p + (4/16)\pi/T_p$ with a range of source positions, in detail, $(x_o, y_o) = (0, 150\text{ m})$, (0, 1150 m), (0, 2150 m), (0, 3150 m) and (0, 4150 m). Other parameters are identical to those of base combination. It is evident that as the source is moved offshore, the main axis of the spreading heat is identically shifted offshore and the maximum excess temperatures near the coast and along the main axis of the heat dispersion are all reduced. Shifting the source position in an offshore direction gives rise to the reduction of the image source contribution in the equation (12). Physically, the shoreline constraint is relaxed, which controls the degree of lateral spreading of the heated water. That is, the one-sided lateral spreading is allowed

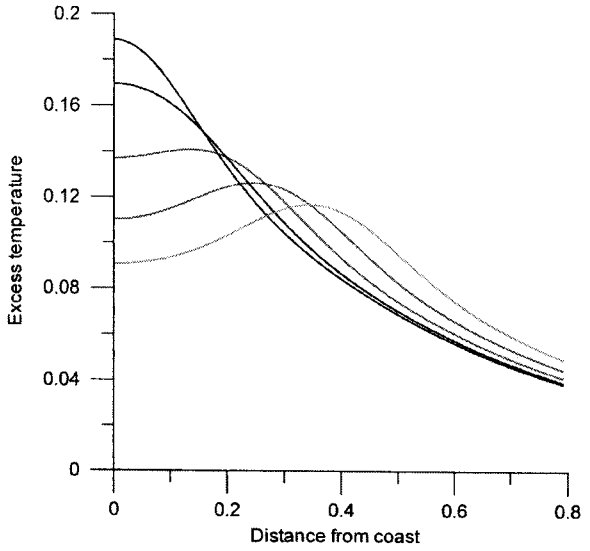

Fig. 3. The distributions of the maximum excess temperature at the cross section of $x = L_{0.8}$ computed at $t = 199T_p + (4/16)\pi/T_p$ with source positions, (x_o, y_o) = (0, 150 m) (black), (0, 1150 m) (blue), (0, 2150 m) (green), (0, 3150 m)(red) and (0, 4150 m) (orange).

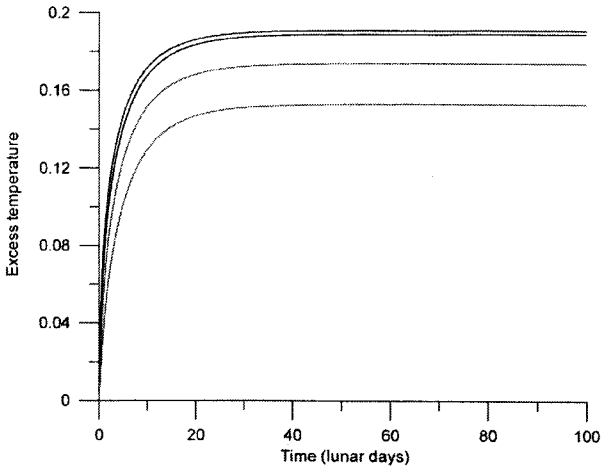

Fig. 4. The maximum excess temperatures at $x = L_{0.8}$ computed with U_{max} = 0.9 m/s (blue), 0.8 m/s (black), 0.75 m/s (green) and 0.7 m/s (red).

when the source is located near the coast, while the two-sided lateral spreading tends to occur when the source is located at the offshore side. As y_o goes to infinity, the image source contribution virtually disappears and the discharge in a semi-infinite ocean will be then identical to the discharge in an open ocean.

From Fig. 3, it is also seen that, while the maximum excess temperatures on the onshore side and along the main axis of the heat dispersion is reduced as a result of the offshore discharge, the excess temperature on the offshore side is gradually increased. It is quite natural because the total heat must be conserved. In reality, however, the tendency on the offshore side can be changed (even reversed) because the water depth usually increases as it goes in an offshore direction. That is, it is possible that an increase in heat capacity might result in a decrease in the excess temperature. The situation can be further complicated when the cross-flow intensity significantly varies.

Effects of changing the intensity of oscillatory alongshore-flow

We examine the sensitivity in heat build-up to the change in cross-flow intensity, keeping in mind that the fortnightly modulation is a distinct feature of the oscillatory flow in real coastal waters. That is, in spring tides, the cross-flow intensifies and in neap tide, the cross-flow weakens.

The maximum excess temperatures computed at $x = L_{0.8}$ with U_{max} = 0.9 m/s, 0.8 m/s, 0.75 m/s, and 0.7 m/s are compared (Fig. 4). We see that increasing the intensity of the cross-flow produces higher excess temperature. It is interesting to note that, comparing these results with U_{max} = 0.9 m/s and 0.8 m/s, calculations with U_{max} = 0.75 m/s and 0.7 m/s give rise to a significant reduction in the maximum excess temperature. The reason can be found in the shoreline distribution of the maximum excess temperature shown in Fig. 2. We see that, as the intensity of the cross-flow alters the excursion distance, $L_{0.8}$ will be located at the inside of the tidal excursion distance estimated from U_{max} = 0.9 m/s, where the shoreline distribution of the heat field reveals a smooth variation, while just outside of the tidal excursion distances estimated at from U_{max} = 0.75 m/s and U_{max} = 0.7 m/s, the shoreline distribution is reduced steeply.

It is important, however, to note that the sensitivity results given here do not guarantee the occurrence of higher shoreline excess temperature in spring tide than at neap tide. This is primarily because the heat field at a specific time is determined as a superposition of past heat release. That is, the heat fields at the previous neap and mid-tide all contribute to the formation of the heat field at spring tide. Similarly, the heat fields in the previous spring and mid-tide all affect the heat field at neap tide. Therefore, the difference in the distribution of heat between spring and neap tides can be significantly less than predicted in Fig. 4 with the assumption being that the cross-flow is maintained with the same intensity throughout

the integration time. Secondly, the fact that the dispersion process is most uncertain might be the reason. Instead of the formulation given in equation (13) in which the degree of turbulent dispersion is assumed to vary linearly according to U_{max}, higher order variation might be possible. For these reasons, chances are such that the conclusion might be even reversed depending upon the parameterization of the dispersion coefficients. Change in water depth with tide of course complicates the situation.

Effects of changing the dispersion coefficients

To examine the sensitivity of the heat build-up to the change in turbulent dispersion, two sets of results are compared with each other. The first set includes results with a range of values of k_x (in detail, with $\theta = 8.4/2$, 8.4/1.5, 8.4 × 1.5 and 8.4 × 2) but with a fixed value of k_y used in base combination ($\theta = 0.84$, $\alpha^2 = 1$). The second set includes the sensitivity calculations with a range of values of k_y (in detail, with $\theta = 8.4/2$, 8.4/1.5, 8.4 × 1.5 and 8.4 × 2) but with a fixed value of k_x used in base combination ($\theta = 0.84$).

The maximum excess temperatures computed at $x = L_{0.8}$ with a range of values k_x (solid lines) and k_y (dashed lines), respectively, are presented in Fig. 5. The result with base combination (that is, $\theta = 0.8$, and $\alpha = 1$) is then compared. It is noted that the maximum excess temperature widely varies according to the change in the values of the dispersion coefficients. It is obvious that the heat field will change more markedly if k_x and k_y vary together. Sensitivity of the heat field to the change of k_x than k_y might be attributed to the effects of shoreline constraint.

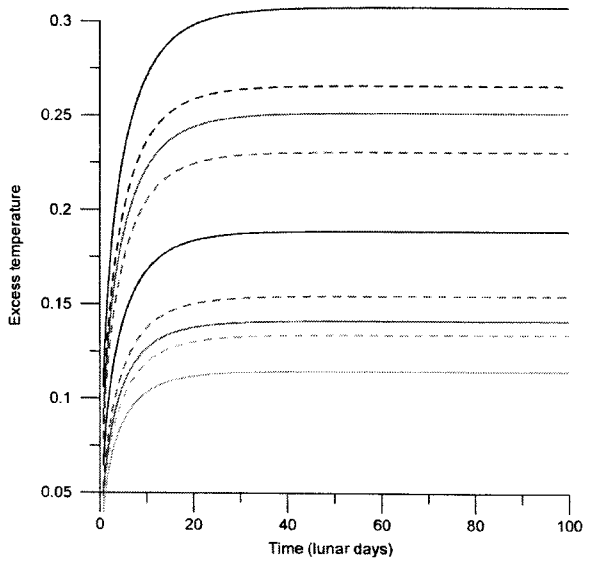

Fig. 5. Time variation in the maximum excess temperatures at $x = L_{0.8}$ computed with a range of values of k_x (with θ = 8.4/2 (blue solid), 8.4/1.5 (green solid), 8.4 (black solid), 8.4 × 1.5 (red solid) and 8.4 × 2 (orange solid)) but with a fixed value of k_y used in base combination, and with a range of values of k_y(with θ = 8.4/2 (blue dashed), 8.4/1.5 (green dashed), 8.4 × 1.5 (red dashed) and 8.4×2 (orange dashed)) but with a fixed value of k_x used in base combination.

The difficulty of choosing a proper value of the horizontal dispersion coefficients is well-known in the modeling communities. A few examples of values used in the thermal studies are as follows. Wada and Kadoyu (1975) examined heat dispersion using the values ranging from 1 m^2/s to 10 m^2/sec with isotropic and non-isotropic assumptions. In the particle tracking model by KEPRI (1993) $k_x = k_y = 1$ m^2/s was used. Bectel Civil and Minerals, Inc. (1982) used 20 m^2/s in finite-element modeling for the Youngkwang nuclear power plant. Pukyung University (1996) adopted $k_x = 60.6$ m^2/s, $k_y = 40.4$ m^2/s, in a three-dimensional modeling of thermal prediction at Youngkwang. Many random values were indeed used. It is emphasized that the uncertainty of the dispersion coefficients mostly limits the accuracy of thermal prediction.

Fig. 6 and Fig. 7 show the successive alongshore distributions of the heat field at four different times of the 200th lunar tidal cycle, as in Fig. 3, computed with θ = 8.4 × 2 and 8.4/2, respectively (fixing k_y as the value used in base combination). As expected, considerable changes are noted. The use of a relatively high value of k_x almost eliminates the bulge-like form previously noted in Fig. 2,

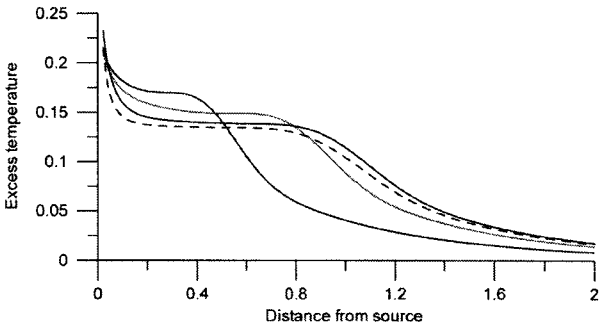

Fig. 6. The instantaneous alongshore distributions of the excess temperature at the four successive time steps of the 200th lunar tidal cycle ($t = 199T_p + (4/16)\pi/T_p$ (blue), $t = 199T_p + (6/16)\pi/T_p$ (green), $t = 199T_p + (8/16)\pi/T_p$ (black solid), and $t = 199T_p + (9/16)\pi/T_p$) (black dashed) computed with θ = 8.4 × 2 (fixing k_y as the value used in base combination).

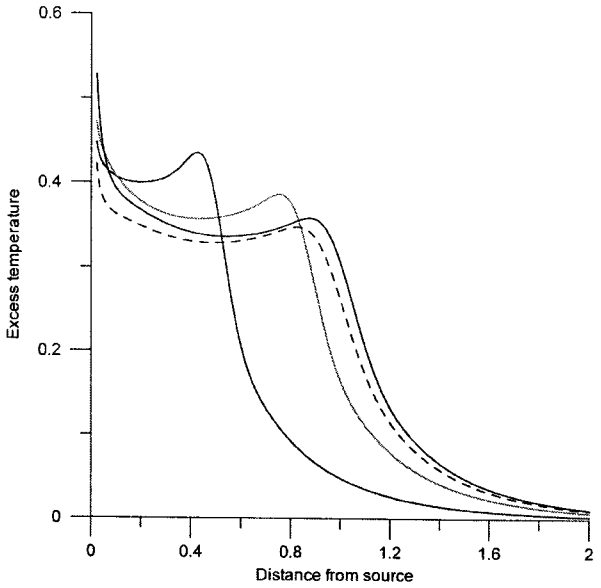

Fig. 7. Same as in Fig. 6 but computed with θ = 8.4/2 (fixing k_y as the value used in base combination).

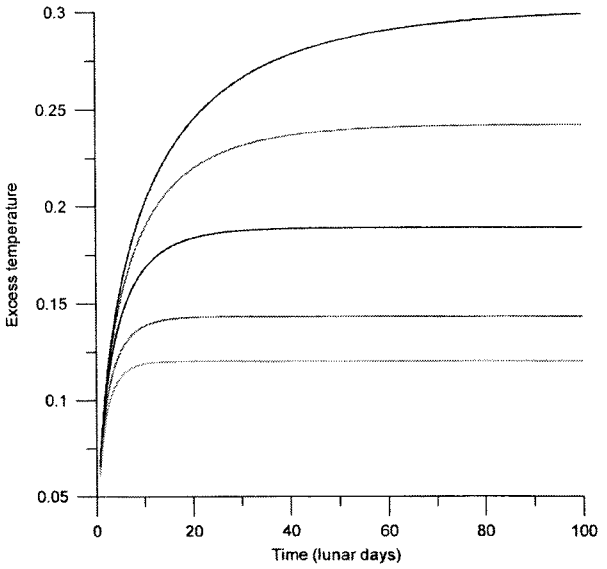

Fig. 8. Time variation in the maximum excess temperatures at $x = L_{0.8}$ computed with a range of values of k_d (= 1/4 × k_{do} (blue), 1/2 × k_{do} (green), k_{do} = 0.1065 × 10^{-5}/s defined in base combination (black), 2 × k_{do} (red) and 4 × k_{do} (orange).

smoothing out the slope on the downstream front side. On the contrary, using a relatively low value of k_x the bulge-like form becomes much more pronounced and the slope on the downstream front side becomes markedly steep. That is, when the tidal convection dominates the dispersion process, the bulge-like form on the downstream front side becomes pronounced. The bulge-like form hardly appears in reality because turbulent mixing is usually intense in the near-field region.

Effects of changing the decay coefficient

Apart from the water exchange with offshore water, the heat field in coastal waters is never in equilibrium with the atmosphere due to the change in meteorological conditions. The decay coefficient is generally known as a function of wind speed, the dew point temperature and sea surface temperature (Edinger *et al.*, 1974). For that, a series of calculations are carried out for a range of values of k_d. In detail, we consider the values of k_d = 1/4 × k_{do}, 1/2 × k_{do}, k_{do} = 0.1065 × 10^{-5}/s (the value defined in base combination), 2 × k_{do} and 4 × k_{do}. Other parameters are identical to those of the base combination.

The decay coefficient k_d is related to the heat loss coefficient k_l as follows:

$$k_d = \frac{k_l}{\rho c_p h} \tag{15}$$

where ρ is water density, and c_p is the specific heat of water. It is noted that, in addition to the meteorological effects, the variation of water depth results in the considerable fluctuation of the decay coefficient with a tidal period in shallow water with a large tidal variation. Note that the value of k_{do} gives k_l = 32 W/m^{2}C^{-1}.

For reference, we summarize values used in other studies. For Youngkwang nuclear power plant, Bectel Civil and Minerals, Inc. (1982) used k_l = 30 W/m^{2}C^{-1}, KEPCO (1992) used 32 to 42 W/m^{2}C^{-1}. KOPEC (2001) and Kunsan University (2002) used 32 and 20 W/m^{2}C^{-1}, respectively, while Pukyung University (1996) chose the value of k_l in winter nine times higher than in summer (the values are not presented here because the unit used is uncertain). KEPRI (1993) used 20 W/m^{2}C^{-1} in a particle tracking modeling of Samchonpo coal-fired plant and values ranging from 20 to 28 W/m^{2}C^{-1} in two-dimensional finite-difference model for Boryong coal-fired power plant.

From Fig. 8, it is, as expected, evident that use of a large value decay coefficient gives rise to fast convergence. By employing a smaller value (k_d = 1/4 × k_{do}), it has been found that the excess temperature still increases, though very marginally after 100 lunar days.

Table 2 summarizes the comparison of time scales for a range of k_d which is required for the heat field ($x = L_{0.8}$, 150 m) to reach a range of percentages of the quasi-

Table 2. Time required with a variation of k_d for the maximum excess temperature at $x = L_{0.8}$ to reach certain percentages of the quasi-steady state value.

$\frac{T_{max}(\ ,t)}{T_{max}(\ ,t_{qs})}$ (in %)	Elapsed time (in lunar days)			
	$k_d = 1/4k_{do}$	$k_d = 1/2k_{do}$	$k_d = 2k_{do}$	$k_d = 4k_{do}$
70	11.7	7.0	2.2	1.6
80	18.9	11.1	3.5	2.5
90	34.0	19.2	5.8	4.2
95	51.2	28.6	8.5	5.9

steady state. In the case of $k_d = 1/4k_{do}$, t_{qs} is chosen as the 150th lunar day, while in other cases as the 100th lunar day.

Again, it is noted that, within the e-folding time scale, the heat build-up occurs up to 90% in terms of the quasi-steady state values in a region within a tidal excursion distance.

We will now consider the effects of time variation in the decay coefficient, keeping in mind that in reality the variation in meteorological conditions persists. For that, it is assumed that the coefficient varies in a pulse form for a finite interval (from t_1 to $t_1 + \Delta T$). That is,

$$\begin{aligned} k_d &= k_{d1} \quad \text{for} \quad t_1 \le t \le t_1 + \Delta T = t_2 \\ &= k_{d2} \quad \text{for the rest of period} \end{aligned} \tag{16}$$

where k_{d1} and k_{d2} are constants.

The excess temperature field is then given by

$$\begin{aligned} T = &\int_0^{t_1} \frac{\alpha q T_o}{4\pi h k_x (t-\tau)} \cdot I(x-x_o, y-y_o, t, \tau) \cdot e^{-k_{d1}(t-\tau)} d\tau \\ &+ \int_{t_1}^{t_2} \frac{\alpha q T_o}{4\pi h k_x (t-\tau)} \cdot I(x-x_o, y-y_o, t, \tau) \cdot e^{-k_{d2}(t-\tau)} d\tau \\ &+ \int_{t_2}^{t} \frac{\alpha q T_o}{4\pi h k_x (t-\tau)} \cdot I(x-x_o, y-y_o, t, \tau) \cdot e^{-k_{d1}(t-\tau)} d\tau \\ &+ (\text{Image source terms}) \end{aligned} \tag{17}$$

Two sets of calculations have been performed. Firstly, we consider a case where the heat loss to the atmosphere is suddenly increased four times (that is, $k_d = 4 \times k_{do}$) from 30 lunar days for 4, 6, 8 and 16 days (for the rest of the periods k_d is assumed to be the same as the base combination). Secondly, we examine the case of heat loss to the atmosphere as being suddenly reduced to one fourth ($1/4 \times k_{do}$) from 30 lunar days for 4, 6, 8 and 16 days (for the rest of the period k_d is, for the sake of convenience, is assumed to be twice that defined in the base combination).

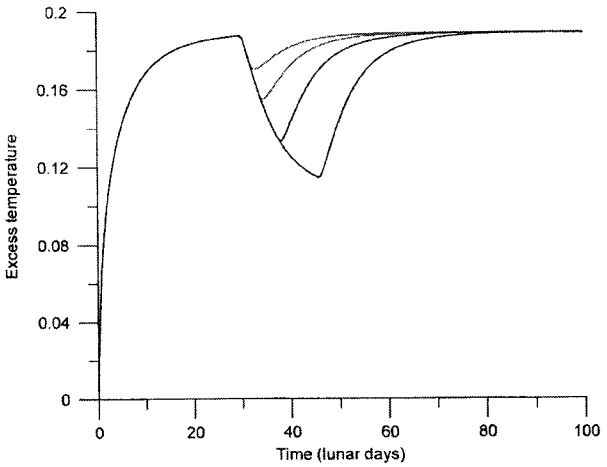

Fig. 9. Time variation in the maximum excess temperatures at $x = L_{0.8}$ computed with a range of values of ΔT (2 days (red), 4 days (green), 8 days (blue) and 16 days (black) during which the heat decay rate is suddenly increased four times (that is, $k_{d1} = 4 \times k_{do}$ from 30th lunar days to 30days + ΔT). For the rest of periods $k_{d2} = k_{do}$ that is, same as in base combination.

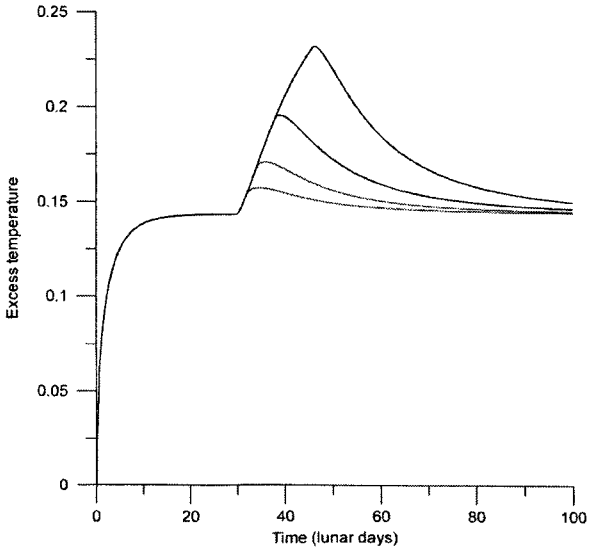

Fig. 10. Same as Fig. 9 but the heat decay rate is suddenly decreased four times (that is, $k_{d1} = 1/4 \times k_{do}$). For the rest of periods $k_{d2} = 2 \times k_{do}$, that is, twice of that defined in base combination.

Fig. 9 and Fig. 10 display the results. It is noted that a time variation in the maximum excess temperature at $x = L_{0.8}$ tends to decrease sharply as the heat decay is

increased. As the heat decay returns to the initial value, the excess temperature gradually increases. Reverse patterns occur in the second case.

4. Discussions

In this study we have examined the time evolution of the heat build-up by using an analytical solution due to a point source. The solution assumes a coastal water with constant water depth, which takes into account the presence of a uniform oscillatory cross-flow with non-isotropic horizontal turbulent dispersion. Some extensions of previous analytical models have been achieved in this study. The model developed by Holley (1969) and also Harleman (1971) has been extended to a two-dimensional model and the limitation of the time invariant property of heat loss to the atmosphere has been partially relaxed by allowing the related coefficient to vary in a step-wise manner. However, considerable limitations still remain, which include the assumption that the amplitude and phase of the oscillatory cross-flow as well as water depth are spatially uniform and that the turbulent intensity is constant in time and space.

Despite the inherent limitations, some valuable features have been found through its application. A series of calculations reveal that the heat build-up due to a specific heat source varies sensitively to the values of basic physical parameters. It has been noted that proper choices of the decay coefficient as well as the dispersion coefficients are most critical to the reliable prediction of the excess temperature field. The dispersion coefficients determine the absolute values of the excess temperature and characterize the alongshore profile, particularly within the tidal excursion distance. The decay coefficient determines the absolute value of the excess temperature and the convergence rate to the quasi-steady state. Calculations with a range of source positions and shoreline-flow intensity provide an insight on the role of a jetty recently constructed as a countermeasure to reduce thermal extension along the coast at the front of the outlet of the Youngkwang Nuclear Power Plant. We know that the jetty effectively guides the discharged heated water to a point offshore. It is therefore rational to assume that the source position is effectively moved to the offshore side. Results obtained in this study indicate that the excess temperature in the direction of the shoreline reduces as the shore constraint is relaxed (in addition, the increase in water depth and dispersion, since proportional to h is also a reason). The sensitivity calculations with a range of values of oscillatory currents indicates that a significant increase in the excess temperature is hardly possible with a local increase in the current field induced by the jetty.

Some comments are also given on the numerical modeling. One of basic question raised in thermal modeling is how long the model integration has to be continued. Our answer is that it is specific problem, but depends primarily upon the local rate of heat decay (which is determined by the heat loss to the atmosphere and water depth). Up to now there have been numerous thermal studies in Korea, but efforts to carry out meterological measurements can hardly be found. Nearby on-land measurements have been used to assess the heat loss rate. However, it should be noted that the in situ meteorological conditions can be considerably different from on-land conditions. Long-term measurements of meteorological conditions have to be performed as an essential part of thermal studies. Furthermore, the definition of heat loss coefficient appears to be clarified. The values applied in the previous studies are too random and the seasonal variation is very questionable. It is finally emphasized that, even in cases where long-term meteorological records are available, the model prediction must be verified through field observations of the heat field because the model cannot avoid numerical noise and errors in representing the dynamic process of heat dispersion. There is of course limitations in accuracy in assessing the excess temperature on the basis of field observations. Interactive use of analytical and numerical models might be a desirable way to obtain reliable estimate of the dramatically excessive temperatures along with extensive field measurements.

We will briefly mention our plans for future study. As a sequel to the present study, heat dispersion in the presence of both mean and oscillatory currents with spring-neap modulation is our immediate concern. Development of a model with assumption of a line source rather than a point source is under progress, which is physically equivalent to somehow taking into account the presence of the jet momentum near the outlet. For the thermal studies in a deeper, stratified coastal sea region, where the vertically well-mixed assumption fails, the extension of the present model to a two-and-a-half (Wada *et al.*, 1975) or three-dimensional model is necessary. Reports on these matters will be followed in the near future.

The solution derived in this study is applicable to other pollutant dispersion problems once a proper choice is made on the term of decay. Applications to dispersion of waste and dredged materials will be reported in the future.

Acknowledgements

The first author has been in part supported by research projects with contract numbers PE83700 and PE38400, while the last author has been supported by a research project with contract number PE83700. Careful readings and comments made by Professor Y. J. Noh, Chungnam University, and Professor Y. K. Cho, Cheonnnam University are very much appreciated.

References

Atkins, R. and C.F.M. Diver. 1975. Mathematical modelling of heated discharges in tidal flow, 2. Plume development and dispersion. Hydraulics Research Station, Report No. INT 147, 16 p.

Bectel Civil and Minerals, Inc. 1982. Numerical hydrothermal study of cooling water discharges and intake temperatures. 93 p.

Carslaw, H.S. and J.C. Jaeger. 1959. Conduction of heat in solids, 2nd edition. Oxford University Press, 510 p.

Carter, H.H. and A. Okubo. 1965. A study of physical processes of movement and dispersion in the Cape Kennedy area. Final Report under the U.S. Atomic Energy Commission, Report no. NYO-2973-1, Chesapeake Bay Institute, The Johns Hopkins Univ., 164 p.

Cussler, E.L. 1984. Diffusion, mass transfer in fluid systems, Cambridge University Press, 525 p.

Edinger, J.E., D.K., Brady, and J.C. Geyer. 1974. Heat exchange and transport in the environment. Cooling Water Discharge Project Report No., 14, Electric Power Research Institute Publication No. 74-049-00-3, Palo Alto.

Harleman, D.R.F. 1971. One dimensional models. p. 34-101. In: *Estuarine Modelling: An Assessment*, eds. by G.H. Ward, Jr., W.H. Epsey, Jr.

Holley, E.R. 1969. Discussion of difference modeling of stream pollution. *J. Sanitary Engineering*, 95, SA5, 968-972.

Hydraulics Research Station. 1975. Mathematical modeling of recirculation of heat, Orfordness Power Station. Hydraulics Research Station Report No. EX 685, 34 p (with 19 figures).

Hydraulics Research Station. 1978. A numerical model for background temperature fields. Hydraulics Research Station Report No. EX 806, 44 p (with 3 Tables and 32 figures).

Jirka, G.H. and S.W. Hinton. 1992. User's guide for the Cornell Mixing Zone Expert System (CORMIX). Technical Bulletin No.624, U.S. Environmental Protection Agency, Athens, Georgia.

Jung, K.T., S.D. Kim, C.W. Park, J.Y. Jin, and J.S. Park. 2002. Far-field prediction of the dispersion of thermal effluents in a shallow coastal sea region using the CORMIX system. *Proceedings of the KOSMEE spring annual meeting*, May 10, 2002, Jeju, 257-263.

KEPCO. 1992. An oceanographic survey report around Youngkwang nuclear power plant. 821 p.

KEPCO. 2001. A reassessment study of countermeasures of reducing thermal impact due to the delay of the construction of Kushipo harbor. 103 p (with three appendices) (in Korean).

KEPRI. 1993. Studies on impact of power plant operation on marine environment at the coastal areas of three coal-fired T/Ps in Korea. *Report* No. KRC-90C-JO3, 336 p (in Korean).

KORDI. 2002. Oceanographic survey in association with the operation of 5 and 6 units of Youngkwang nuclear power plant. *Interim reports* I and II (in Korean) (unpublished manuscript).

Kunsan University. 2002. Thermal impact study on Kochang area due to the construction and operation of 5 and 6 units of Youngkwang nuclear power plant. Interim report, 58 p (in Korean) (unpublished manuscript).

Okubo, A. 1967. The effect of shear in an oscillatory current on horizontal diffusion from an instantaneous source. *Int. J. Oceanogr. and Limnol.*, 1, 194-204.

Pukyung University. 1996. Oceanographic environmental survey report on coastal areas around Youngkwang nuclear power plant. 663 p (in Korean).

Talbot, J.W. 1973. Measurement of dispersion. Water Pollution Research, Technical report, No., 13, HMSO.

Wada, A. and M. Kadoyu. 1975. Proposal of computation chart for general use for diffusion prediction of discharged warm water. *CRIEPI Report* No. 375008, 65 p.

Wada, A., N. Katano, M. Kadoyu, and H. Araki. 1975. Study on adaptability of prediction method of simulation analysis for diffusion of discharged warm water in the sea. *CRIEPI Report* No. 73001, 88 p.

Yasuda, H. 1982. Longitudinal dispersion due to the boundary layer in an oscillatory current: theorectical analysis in the case of an instantaneous line source. *J. Oceanogr. Soc. Japan*, 38, 385-394.

Received Jan. 9, 2003
Accepted Mar. 15, 2003

Appendix: Derivation of the basic equation governing the excess temperature

The derivation of the basic equation governing the excess temperature field is described below with emphasis on the underlying assumptions. The heat balance equation may be written in the following form

$$\frac{\partial T}{\partial t} + u\frac{\partial T}{\partial x} = k_x\frac{\partial^2 T}{\partial x^2} + \frac{k_x}{\alpha^2}\frac{\partial^2 T}{\partial y^2} + \frac{Q_n}{\rho c_p h} \quad \text{(A1)}$$

where Q_n is the net heat exchange between the sea and atmosphere.

Representing the heat exchange via the concept of equilibrium temperature, T_e, that is,

$$Q_n = -1/(\rho c_p h)\cdot(T - T_e) = -k_d(T - T_e) \quad \text{(A2)}$$

equation (A1) reduces to

$$\frac{\partial T}{\partial t} + u\frac{\partial T}{\partial x} = k_x\frac{\partial^2 T}{\partial x^2} + \frac{k_x}{\alpha^2}\frac{\partial^2 T}{\partial y^2} - k_d(T - T_e) \quad \text{(A3)}$$

The ambient temperature field, the heat field in the absence of heat source, may be written in a similar form.

$$\frac{\partial T_a}{\partial t} + u_a\frac{\partial T_a}{\partial x} = k_x\frac{\partial^2 T_a}{\partial x^2} + \frac{k_x}{\alpha^2}\frac{\partial^2 T_a}{\partial y^2} - k_d(T_a - T_e) \quad \text{(A4)}$$

Strictly speaking, the turbulent diffusion coefficients, the decay coefficient and the equilibrium temperature are all different from those with heat discharge, but is assumed, without loss of generality, to remain unaltered.

Subtracting equation (A4) from equation (A1) leads to

$$\frac{\partial(T - T_a)}{\partial t} + u\frac{\partial T}{\partial x} - u_a\frac{\partial T_a}{\partial x} = k_x\frac{\partial^2(T - T_a)}{\partial x^2} + \frac{k_x}{\alpha^2}\frac{\partial^2(T - T_a)}{\partial y^2} - k_d(T - T_a) \quad \text{(A5)}$$

Assuming that $u = u - \Delta u$, equation (A5) can be written as

$$\frac{\partial(T - T_a)}{\partial t} + u\frac{\partial(T - T_a)}{\partial x} + \Delta u\frac{\partial T_a}{\partial x} = k_x\frac{\partial^2(T - T_a)}{\partial x^2} + \frac{k_x}{\alpha^2}\frac{\partial^2(T - T_a)}{\partial y^2} - k_d(T - T_a) \quad \text{(A6)}$$

Introducing the excess temperature,

$$\Delta T = T - T_a \quad \text{(A7)}$$

and assuming that Δu is smell and

$$\frac{\partial T_a}{\partial x} \ll \frac{\partial \Delta T}{\partial x} \quad \text{(A8)}$$

we finally get

$$\frac{\partial \Delta T}{\partial t} + u\frac{\partial \Delta T}{\partial x} = k_x\frac{\partial^2 \Delta T}{\partial x^2} + \frac{k_x}{\alpha^2}\frac{\partial^2 \Delta T}{\partial y^2} - k_d\Delta T \quad \text{(A9)}$$

It is noted that the above equation does not includes the equilibrium temperature. The condition of (A8) implies that the application of equation (A9) can produces a biased solution in a frontal region. The same is true in a three-dimensional case whenever the ambient water is strongly stratified.